EXPERIMENTAL STUDY ON CRACK BRIDGING IN FRC UNDER UNIAXIAL FATIGUE TENSION

By Jun Zhang,[1] Henrik Stang,[2] and Victor C. Li,[3] Fellow, ASCE

ABSTRACT: This paper presents an experimental study on crack bridging in steel-fiber-reinforced concrete (SFRC) materials under deformation-controlled uniaxial fatigue tension. Two types of commercially available steel fibers, straight steel fiber and hooked end steel fiber, were used separately in this experimental investigation. A total of six series of fatigue tensile tests with constant amplitude between maximum and minimum crack openings were conducted. The experimental results show that the bridging stress decreases with the number of load cycles, and this phenomenon is termed bridging degradation. The general behavior of the bridging degradation with the number of cycles in SFRCs is represented by a fast dropping stage (reduction in bridging stress within the first 10–15 cycles) with a decelerated degradation rate, followed by a stable stage with an almost constant degradation rate for straight SFRC, or by several periods with a decelerated rate in each period for hooked SFRC. Although fiber deformation, such as in hooked end fiber, can improve the monotonic crack bridging significantly, faster bridging degradation is found in hooked SFRC than in straight SFRC with the same maximum crack width (>0.1 mm) and minimum load condition.

INTRODUCTION

Interest in fatigue performance of concrete began at the end of the last century with the development of reinforced concrete railroad bridges. These bridges are expected to resist millions of cycles of repeated axle loads from passing traffic during their service life. In a reinforced concrete member subjected to bending moment, the internal resisting couple consists of a tensile force contributed by steel and a compressive force provided by the concrete. Consequently, fatigue failure occurs either in tension in the reinforcing steel or in compression in the concrete. The development of highway systems in the 1920s led to further interest in the fatigue of concrete. Concrete pavements for highways are subjected to millions of cycles of repeated axle loads from trucks and automobiles. Airport pavements are subjected to a smaller number of loading cycles during their designed life ranging from about several thousand to several hundred thousand cycles of repeated loading. Since concrete pavements are usually unreinforced, concrete is expected to resist tension and consequently knowledge of fatigue performance in tension is also needed. Concrete structures supporting dynamic machines are also subjected to hundreds of millions of load cycles involving complicated stress states. Serious fatigue problems are related to such structures. Numerous studies have been made in the past to evaluate the fatigue performances of plain concrete (Tepfers and Kutti 1979; Hsu 1981; Gylltoft 1983; Saito and Imai 1983; Hordijk 1991; Byung and Oh 1986).

Incorporation of steel or other fibers in concrete has been found to improve several of its properties, primarily cracking resistance, impact and wear resistance, and ductility. For this reason fiber-reinforced concrete (FRC) is now being used in increasing amounts in structures such as airport pavements, highway pavements, bridge decks, machine foundations, and storage tanks. Thus, the fatigue performance of FRC materials must be investigated because of the described reasons. As a relatively new material, the history of investigation on the fatigue of FRC is limited. Experimental evaluations of this behavior have been done in recent years (Ramakrisan et al. 1987; Otter and Naaman 1988; Johnston and Zemp 1991; Stang and Zhang 1994; Zhang and Stang 1998). To date, fatigue life prediction and design of FRC structures have been done mainly through an empirical approach. This type of approach requires time-consuming test data collection and processing for a broad range of design cases that, in principle, are not applicable to other design cases. Therefore, a micromechanics-based fatigue model that is capable of both predicting the fatigue life for a given FRC structure and designing an FRC material for a given fatigue life needs to be constructed (Li and Matsumoto 1998).

Recent theoretical studies (Cox and Rose 1994; Evans et al. 1995; Zhang and Stang 1997a; Li and Matsumoto 1998) have revealed that the rate of fatigue crack growth in a number of different materials, which exhibit crack bridging, is highly dependent on the crack bridging law governing the zone behind the matrix crack and on the law governing the degradation of the crack bridging with the number of load cycles. Thus, the study on the cyclic crack bridging behavior of FRC materials becomes fundamental work in the fatigue investigations of FRC structures. At present, no experimental data are available to describe the degradation of the fiber bridging law of cementitious materials under cyclic loading. Normally it can be assumed that the degradation of the bridging stress is related primarily to degradation of the interfacial bond between fiber and matrix, even though other mechanisms can be present, such as fatigue failure of the fibers in tension/bending during crack opening or fatigue in the fibers in compression/bending during crack closing and subsequent fiber buckling (Wu et al. 1994). The major objective of the present work is to experimentally investigate the bridging behavior of steel-fiber-reinforcing concrete (SFRC) under uniaxial fatigue tension. In this study, a series of deformation controlled fatigue tensile tests with constant amplitude between maximum and minimum crack openings were carried out on two side prenotched specimens. Two types of SFRCs, reinforced with commercially available smooth and hooked steel fibers, respectively, are investigated. The complete relationship between bridging stress and the number of load cycles is obtained. Furthermore, the fundamental bridging degradation law in SFRCs is suggested. Finally, the mechanism of the bridging degradation under fatigue tension is discussed.

[1]Postdoctoral Res. Fellow, Advanced Civ. Engrg. Mat. Res. Lab., Dept. of Civ. and Envir. Engrg., Univ. of Michigan, Ann Arbor, MI 48109-2125.

[2]Assoc. Prof., Dept. of Struct. Engrg. and Mat., Tech. Univ. of Denmark, DK2800, Lyngby, Denmark.

[3]Prof. and Dir., Advanced Civ. Engrg. Mat. Res. Lab., Dept. of Civ. and Envir. Engrg., Univ. of Michigan, Ann Arbor, MI.

Note. Associate Editor: Nemkumar Banthia. Discussion open until July 1, 2000. To extend the closing date one month, a written request must be filed with the ASCE Manager of Journals. The manuscript for this paper was submitted for review and possible publication on September 1, 1998. This paper is part of the ***Journal of Materials in Civil Engineering***, Vol. 12, No. 1, February, 2000. ©ASCE, ISSN 0899-1561/00/0001-0066–0073/$8.00 + $.50 per page. Paper No. 19170.

EXPERIMENTAL PROGRAM

Determination of Bridging Stress under Uniaxial Tension

One of the best ways to determine crack bridging is through a displacement controlled uniaxial tensile test, loaded between parallel traveling end plates. Based on this idea, a testing method for measuring the stress-crack width relationship developed by Stang and Aarre (1992) is used in the present investigation, and a two side prenotched prismatic specimen is adopted. The test setup and the geometry of the test specimen are shown in Fig. 1.

On the requirements of the test equipment and the size of specimen for uniaxial tension, detailed discussions are made by Aarre (1992). The present specimen satisfies the requirements for obtaining a stable test result. The test takes place in specially designed grips, one fixed to the load cell and the other fixed to the actuator piston with standard Instron fixtures. The grips consist of a permanent part and an interchangeable steel block, which is fixed to the permanent part through four bolts. The specimen is glued to the blocks. The glued surfaces of the interchangeable steel blocks and the specimen are sandblasted before gluing to enhance the bond between steel and specimen. By having a large number of such steel blocks, multiple specimens can be tested continuously as it is not necessary to clean the steel blocks after each test. As soft connections between the interchangeable steel blocks and machine are eliminated, the setup takes full advantage of the stiffness of the machine frame. Hereby, it should be ensured that the rotational stiffness of the test setup is large compared with the rotational stiffness of the concrete specimen. A fast curing polymer that attains 90% of its maximum strength in about 4 min was used. The deformation was measured using two standard Instron extensometers (type 2620-602) with 12.5-mm gauge length mounted across each of the two 9-mm-deep and 3-mm-wide notches. The tests were performed in a 250-kN load capacity, 8500 Instron dynamic testing machine equipped for closed-loop testing.

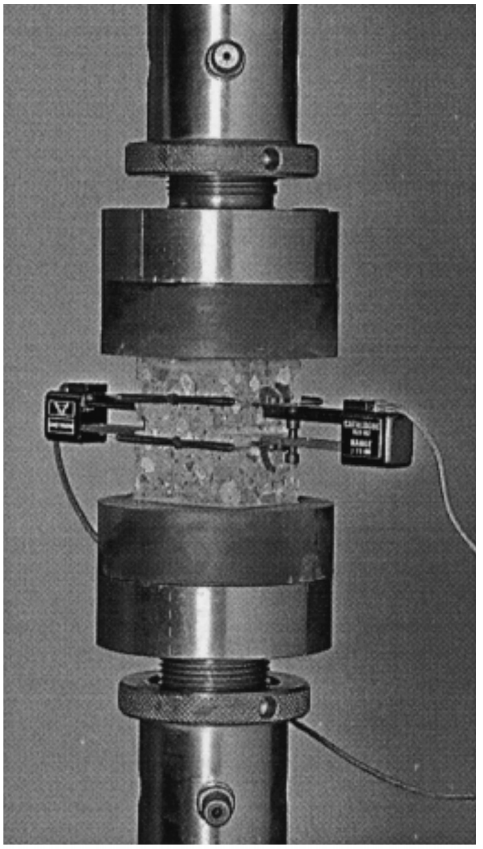

(a)

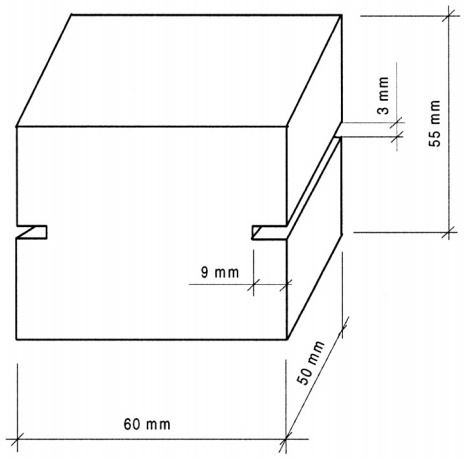

(b)

FIG. 1. Schematic View of Test Setup for Uniaxial Tension and Geometry of Specimen

Loading History and Data Acquisition

The uniaxial fatigue tensile test was conducted under displacement control with a constant amplitude between maximum and minimum crack widths. The minimum crack width value was obtained by a single loading-unloading tensile test at which the bridging load is equal to zero on the unloading branch. The fatigue test commenced with a ramp to the minimum crack value at a rate of 0.01 mm/s followed by a sine waveform fatigue loading in deformation control. To control the accuracy of the maximum crack width value, different load frequencies of 0.25 Hz in the first two cycles and 3.5 Hz for all the rest of cycles were adopted. This fatigue load procedure is shown in Fig. 2.

In this study, a total of six series of fatigue tests with different maximum crack widths was carried out on each of the two types of SFRCs. The selected maximum crack widths were 0.05, 0.10, 0.20, 0.30, 0.40, and 0.50 mm. Because the minimum crack width was determined by a single repeat-loading tensile test, this single deformation controlled loading-unloading tensile test was carried out first. In this test, the specimen was first loaded to a certain maximum crack width starting from 0.05 mm, and then unloaded to zero load; the crack width at zero load was the minimum crack width cor-

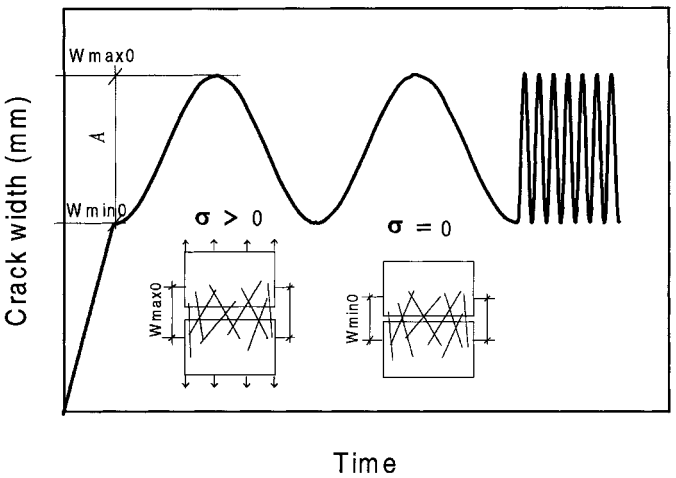

FIG. 2. Deformation-Time Diagram in Fatigue Test

responding to the maximum crack width. After that, the specimen was reloaded to a new maximum crack width until all of the minimum crack width values corresponding to maximum crack widths were obtained. This single loading-unloading tensile test was conducted with a prescribed deformation rate of 1.667×10^{-4} mm/s using the average signal from the two extensometers as feedback.

In the fatigue tensile tests, a special data sampling procedure with an acquisition speed of 16.67 kHz was developed. The data sampling intervals were (1) cycle by cycle in the first 100 cycles; (2) one out of every 30 cycles until 1,000 cycles; (3) one out of every 300 cycles until 10,000 cycles; and (4) one out of every 3,000 cycles until 100,000 cycles. The total number of loading cycles is 10^5. All of the tests were performed in a 250-kN-load-capacity, 8500 Instron dynamic testing machine equipped for closed-loop testing.

Details of Materials, Specimens, and Mixing Procedure

In the present investigation, two types of commercially available steel fibers, smooth and hooked-end, with circular cross sections, 0.4 and 0.5 mm in diameter, 25 and 30 mm in length, respectively, were used separately in the same matrix. A rapid hardening cement, natural sand, and stone with maximum particle size of 4 and 8 mm, respectively, were used. The concrete mix is shown in Table 1.

All prenotched specimens were cut out of beams, 50 mm in width, 100 mm in depth, and 350 mm in length. The mixing procedure can be described as follows. First, the fine and coarse aggregates were mixed together with 1/3 of the total required water. Next, the cement was added, followed by the remaining 2/3 of the water with the supperplasticizer mixed in, and the mixing was continued for 3 min. Then, the steel fibers were gradually spread into the mixer by hand. After that, all of the ingredients were mixed for another 5 min. Then, the fresh concrete was cast into a waterproof plywood mold with inner dimensions of $50 \times 100 \times 350$ mm. After finishing the surface, the surface of specimens was covered with a plastic sheet and cured for 24 h at room temperature. Then, the beams were removed from their molds and put into water with 23°C for 2 months. Afterward, the free surface of casting was cut away to a depth of 40 mm with a water-cooled concrete cutting saw, and the remaining part was further cut into notched specimens, which then were stored in air for another 2 weeks before testing.

EXPERIMENTAL RESULTS AND DISCUSSIONS

Single Loading-Unloading Tensile Tests

The typical single loading-unloading tensile test results, in terms of stress-crack width diagrams, on both smooth steel-fiber-reinforced concrete (SSFRC) and hooked steel-fiber-reinforced concrete (HSFRC), are shown in Fig. 3. The deformation A is the difference between the maximum crack width at which unloading starts and the residual crack width at zero loads. Here A is defined as the reverse slippage due to elastic retraction on fiber and aggregate unloading. We simply call A the reversible deformation or elastic deformation during cyclic loading. Fig. 4 displays the relationship between A and maximum crack width for these two types of SFRCs.

TABLE 1. Mix Proportions of Steel Fiber Concrete

Component (1)	Value (2)
Cement	500 kg/m^3
Sand (maximum particle size 4 mm)	810 kg/m^3
Gravel (maximum particle size 8 mm)	810 kg/m^3
Superplasticizer (66% water content)	3.25 kg/m^3
Water	237.5 kg/m^3
Smooth or hooked steel fibers	78.4 kg/m^3
Fiber volume content V_f	1%

First, the results given in Fig. 3 show typical hysteresis phenomena in the unloading and reloading curves. Second, the bridging stress at unloading points decreases after this single repeated loading procedures. This phenomenon is so-called stress degradation that has been reported for ceramic-based FRC (Rouby and Reynaud et al. 1993; Zhang and Stang 1997b). The bridging stress degradation in FRCs will be presented more clearly in the following presentation of the results of fatigue tests. Fig. 4 shows that the reversible deformation A under cyclic tension is a function of the maximum crack width when the minimum crack width corresponds to the zero loads on the unloading branch. The difference in deformation A between SSFRC and HSFRC gradually increases with the maximum crack width. For SSFRC, a maximum reversible deformation appears around the maximum crack width of 0.1–0.2 mm. According to the pullout mechanism of straight fiber, the maximum reversible slippage will, in theory, appear at the full-debonding point. Before that, it increases with the fiber slippage due to growth of the debonding length. After that, it decreases as a result of the fiber pullout. The present result is consistent with theory. For HSFRC, the reversible deformation increases with maximum crack width. Within the experimental range (i.e., maximum crack width from 0 to 0.5 mm), no peak value is found. It is assumed that the hooks increase the pull-out-loading capacity that will also increase the reversible slippage as unloading. The experimental results shown in Fig. 4 will be referred to later to explain the difference on crack bridging degradation between SSFRC and HSFRC materials.

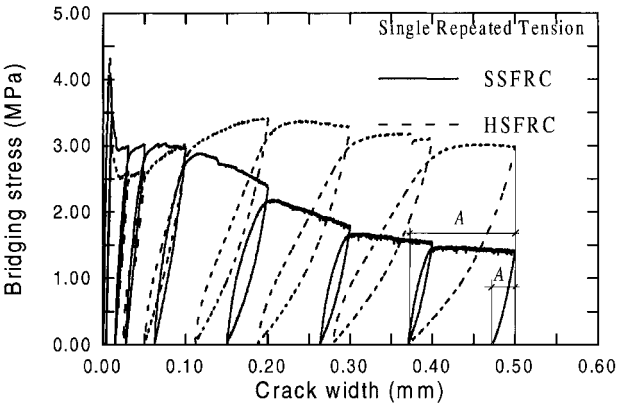

FIG. 3. Typical Stress-Crack Width Curves of Single Repeated Tensile Tests

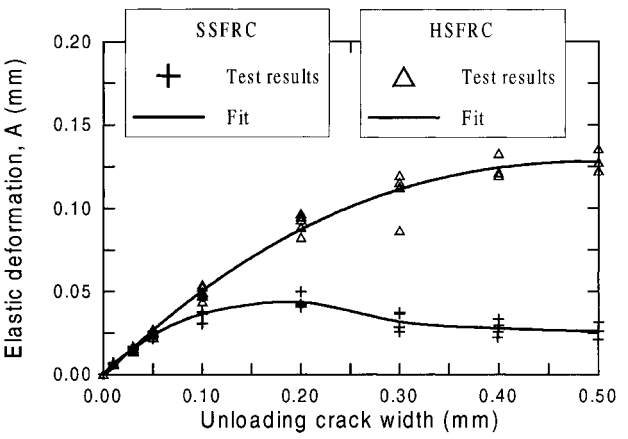

FIG. 4. Elastic Deformation versus Unloading Crack Width

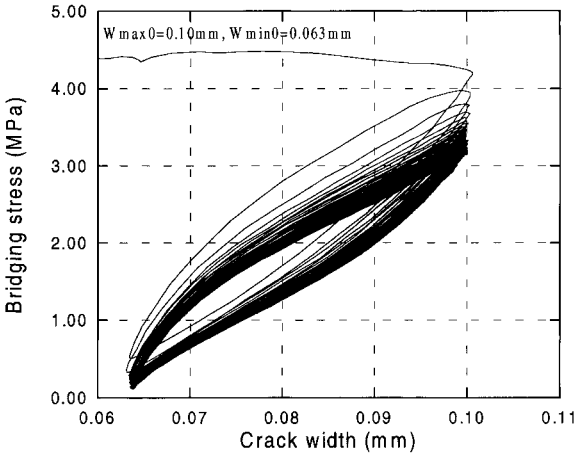

FIG. 5. Typical Stress-Crack Width Curve of Fatigue Tensile Test

The complete experimental results of the single repeated tensile tests can be found elsewhere (Zhang 1998).

Fatigue Tensile Tests

The fatigue tensile test results on the SSFRC and HSFRC materials are shown in Figs. 5 and 6. Fig. 5 demonstrates a typical bridging stress-crack width curve (load-unload loops) during fatigue loading under deformation control on SSFRC specimen. Fig. 5 shows that the secant stiffness $\Delta\sigma/\Delta W$ of reloading branches reduces gradually with the number of load cycles; therefore, the bridging stress at the maximum crack width decreases gradually. The diagrams of bridging stress at maximum crack width versus number of load cycles under different maximum and minimum crack widths (W_{max0} and W_{min0}) are shown in Figs. 6(a–f), where the results in the range of $1–10^5$ cycles are displayed on the right-hand-side of the figures and those in the range of $1–10^2$ cycles are displayed on the left-hand-side of the figures. Here, the maximum bridging stress is normalized with the maximum stress at first cycle, and the average result of all of the individual tests is displayed

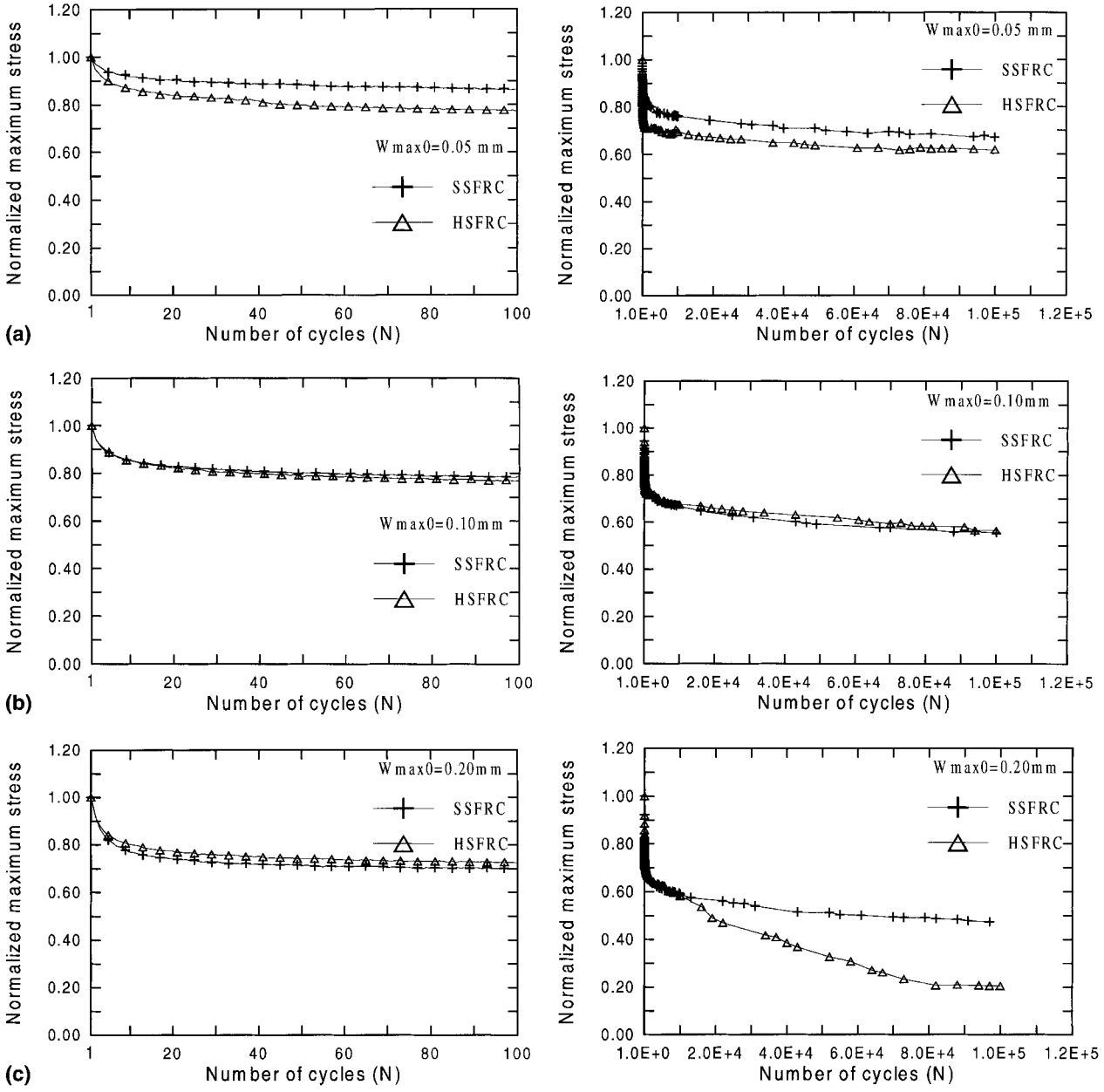

FIG. 6. Relations of Normalized Maximum Bridging Stress and Number of Fatigue Cycles

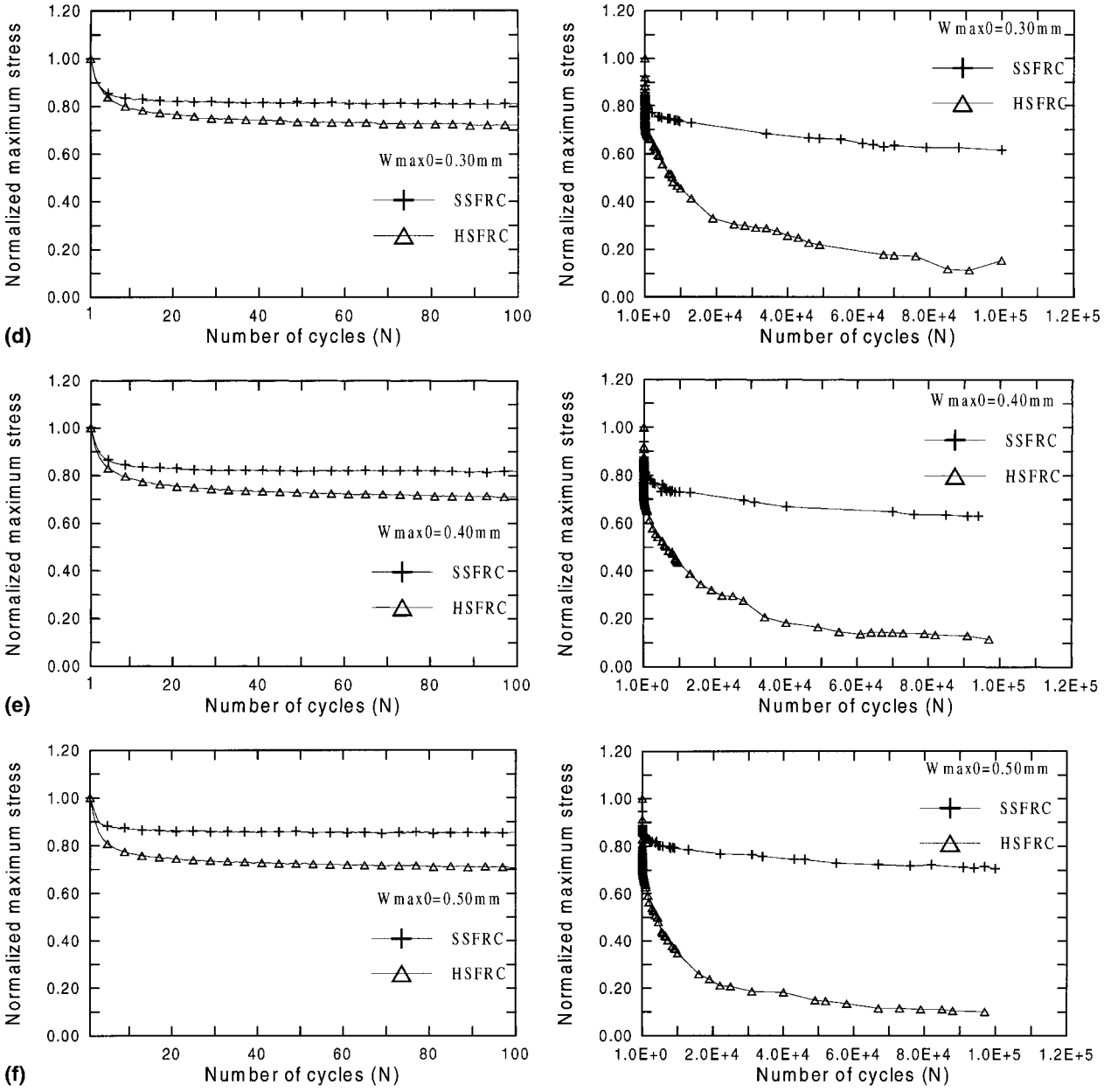

FIG. 6. (*Continued*)

only. The complete test results of all the individuals on both SFRCs can be found in the report by Zhang (1998).

From these results, it is evident that the maximum bridging stress decreases with number of fatigue cycles for both SFRCs under deformation-controlled fatigue load. The behavior of this stress degradation in SSFRC material can be generalized as a fast dropping stage (within the first 10–15 cycles) with a decelerated rate of stress degradation followed by a stable decreasing stage with an almost constant degradation rate within the experimental period. The bridging stress reduces 7, 15, 23, 17, 16, and 13% of their original values when the maximum precracked values are 0.05 mm and 0.10–0.50 mm, respectively, after 10 cycles. This indicates that the rate of bridging decay is affected by the maximum crack width, as shown in Fig. 7, showing here the relations between maximum stress normalized with maximum stress at first cycle and maximum crack width, after 10, 10^2, and 10^5 cycles, respectively. According to the results presented in Fig. 7, it can be seen that the largest stress degradation in SSFRC occurs at a certain point of the maximum crack width between 0.1 and 0.2 mm. Before this peak, the larger the maximum crack width, the larger the stress decay. After that, it is the opposite. Now, comparing Fig. 4 and Fig. 7, it is easy to find that the relationship between elastic slippage-maximum crack width and stress degradation-maximum crack width are very consistent with each other; that is, the larger the elastic slippage, the larger the stress degradation. The largest reduction on crack bridging stress can be >50% of its original value after 10^5 cycles.

For HSFRC, the stress degradation behavior under fatigue tension is different from that of SSFRC. When the maximum crack width is ≤0.10 mm, the behavior of crack bridging degradation is quite similar to that of SSFRC; that is, a fast dropping stage (within first 10–15 cycles) with a decelerated degradation rate followed by a stable decreasing stage with an almost constant degradation rate within the experimental period. The difference in crack bridging degradation between SSFRC and HSFRC is very limited under the same maximum crack width level with the same number of cycles [Figs. 6(a and b)]. However, when the maximum crack width is >0.1 mm, the stress degradation in HSFRC is more pronounced than that in SSFRC [Figs. 6(c–f)]. This means that the reduction on material toughness due to cyclic loading is more sig-

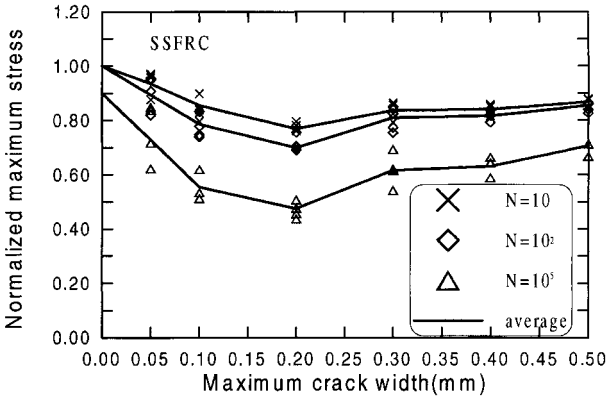

FIG. 7. Relations of Normalized Maximum Bridging Stress and Maximum Crack Width of SSFRC, Showing Results after 10, 10^2, and 10^5 Cycles, Respectively

nificant in HSFRC than that in SSFRC. In these cases, the stress degradation relation in HSFRC material cannot be described simply by two stages.

The bridging degradation process with number of cycles for HSFRC will be divided into more than two stages according to the number of cycles experienced. In each stage, an almost constant rate of bridging degradation can be found, which is much higher than that of SSFRC. Furthermore, a saturation point of bridging degradation in HSFRC seems to exist. From this point, the bridging stress is almost a constant with the number of cycles. The saturation point moves gradually forward with the increase of maximum crack width (e.g., for maximum crack widths of 0.30, 0.40, and 0.50 mm, the determined saturation point of bridging degradation is around 8.5×10^4, 6.0×10^4, and 5.0×10^4 cycles, respectively). The largest crack bridging degradation can be >80% of its original value after 10^5 cycles. In addition, as in the case of SSFRC, the rate of bridging degradation with number of cycles in HSFRC is also affected by the maximum crack width, as shown in Fig. 8. This figure displays the relations between maximum stress normalized with maximum stress at first cycle and the maximum crack width, after 10^1, 10^2, and 10^5 cycles, respectively. From this, we can see that there is no peak point of stress degradation in HSFRC within the experimental range.

Furthermore, through comparing Figs. 4, 7, and 8, a reasonable agreement between the reversible deformation (i.e., the amplitude of deformation controlled fatigue test) and the bridging stress degradation can be found. Apparently, the crack bridging degradation is proportional to the reversible deformation. Thus, in the case of the varied fatigue load condition, this stress degradation could be assumed to be proportional to the accumulated reversible deformation.

Mechanism Analysis of Bridging Degradation

From the experimental results described above, we can conclude that the bridging fibers and aggregates in cement-based composites suffer from fatigue damage, exhibiting the bridging stress degradation with number of fatigue cycles. As we know, the crack bridging in FRC materials is achieved by the bond acting on the interfaces between fiber, aggregate, and the surrounding matrix. The structural performance of fiber-reinforced brittle matrix composites is strongly influenced by the bond behavior of fiber/matrix and aggregate/matrix interfaces. Therefore, the bond characteristic in fiber-reinforced composites can be considered a fundamental material property. Generally, there are two mechanisms of bond between fiber or aggregate and brittle matrix, defined as chemical adhesion and mechanical friction.

Aggregate bridging degradation in concrete under single cyclic uniaxial tension was investigated by Gylltoft (1983), Gopalaratnam and Shah (1985), Reinhardt et al. (1986), and Hordijk (1991). In their studies, similar tensile tests to the current single repeated tension were carried out on plain concrete. The details on concrete mixes, specimens, and test conditions can be found in the original publications quoted above. Figs. 9 and 10 show the relevant results on aggregate bridging degradation. Fig. 9 presents the maximum stress reduction normalized with the stress of unloading start point for different unloading points after this single repeated tensile procedure. Here, the minimum load is equal or close to zero. Fig. 10 displays the elastic (reversible) deformation during unloading-reloading

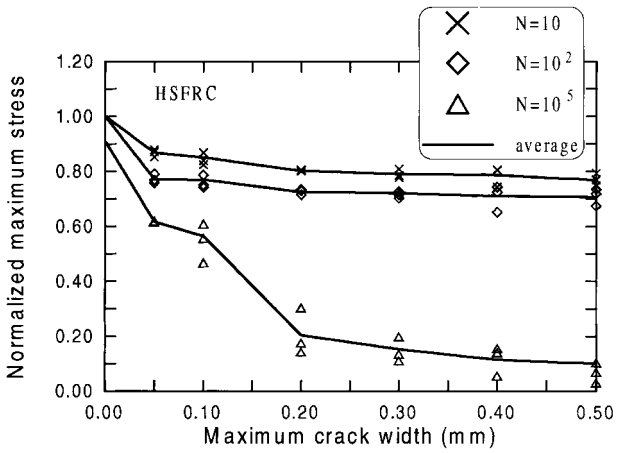

FIG. 8. Relations of Normalized Maximum Bridging Stress and Maximum Precracked Value of HSFRC, Showing Results after 10, 10^2, and 10^5 Cycles, Respectively

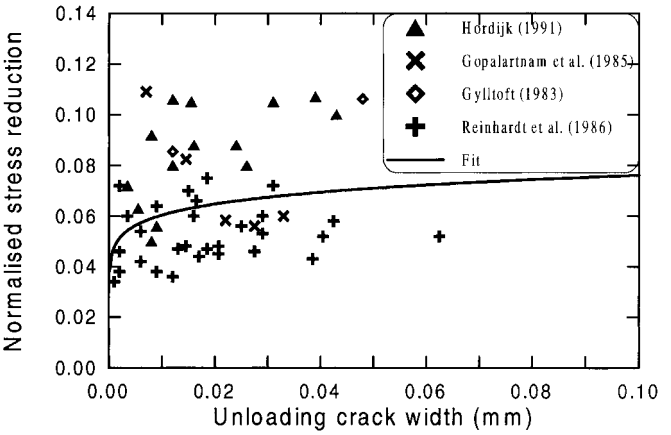

FIG. 9. Normalized Aggregate Bridging Degradation at Different Unloading Crack Width Levels in Single Cyclic Tensile Tests

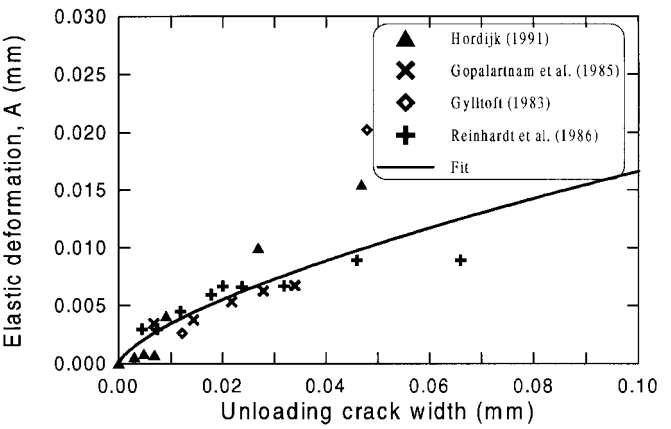

FIG. 10. Elastic Deformation versus Maximum Crack Width Level for Plain Concrete

process as a function of maximum crack width, similar to the curves shown in Fig. 4. Although the test results shown in Fig. 9 have large scatter, the tendency exists that the aggregate bridging degradation increases with maximum crack width. This is consistent with the relationship between elastic deformation and maximum crack width shown in Fig. 10. These experimental findings can be explained with the micromechanics of interfaces between aggregates and matrix as follow. Under cyclic tensile load, the aggregates, which are bridging a crack, undergo a pullout and slip-back process. These reversed movements will smooth the interfaces, which in turn leads to the reduction on the frictional based aggregate/matrix bond strength. Therefore, first, the bond decay is cycle-dependent. It increases with number of load cycles. Second, the amount of this frictional-based bond degradation is proportional to the slippage amplitude of aggregate during cyclic loading, which is represented by the elastic deformation.

Similar mechanisms can be applied to explain the steel fiber bridging degradation under fatigue tension. Loading-unloading processes will cause fiber pullout and slip-back movements. During unloading, the pullout fibers will try to slip-back into the matrix, and therefore a special zone will be created in which the bond stress acts in the reverse direction (Wu et al. 1994). This reversed movement will also gradually wear out the roughness of the interfacial area that results in the frictional-based bond of fiber/matrix interface degradation. This bond degradation is exhibited as the fiber bridging degradation shown in the present fatigue tests. First, the bond degradation of fiber/matrix interface is a function of the number of load cycles, as shown in Fig. 6. Second, the rate of bond degradation is dependent on the reversed slippage of the fibers during cyclic loading, represented by the elastic deformation during cyclic loading (Figs. 7 and 8). The larger the elastic deformation, the larger the bond degradation.

Based on these understandings, it is not difficult to explain the differences on crack bridging degradation laws between SSFRC and HSFRC materials.

Consider a smooth and hooked end single fiber with otherwise-same geometry during pullout from the matrix. The same constant shear stress, so-called bond strength, is assumed to act alone on the debonding interface in both of the fibers. Before full debonding of the fibers, there is the same cyclic pullout behavior between smooth and hooked fibers. Therefore, the same bond degradation will occur on both of fibers under cyclic pullout load because the same loading condition is used. After full debonding, the hooks start to play a rule on crack bridging, and the different cyclic pullout situations between smooth and hooked fibers will occur.

When the fibers are pulled to a deformation level of fiber exit-end slippage δ, corresponding to the onset at pullout of the fiber, the strain distribution in the fiber along the embedded length is shown as lines OE and AB, respectively, for smooth and hooked fibers, which are shown individually in Fig. 11. When unloading to zero load, a zone is created due to unloading where the same amount of interfacial frictional stress acts in the reversed direction to resist fiber moving back to matrix. The length of this reversing zone is a function of the unloading level as well as the initial bond strength (Fig. 11). The amplitude of fiber slippage when unloading to zero can be calculated as the area of CDE and CFB, respectively, for smooth and hooked fibers labeled as S_{CDEC} and S_{CFBC}. For smooth fiber, the amplitude of fiber slippage under cyclic tensile load depends on the bond stress and debonding length or embedded length only. It is proportional to the bond strength, debonding length (before full debonding), or embedded length (after full debonding). The maximum amplitude of fiber pullout and slip-back will appear at the point of full fiber debonding, and the maximum bridging degradation will also appear

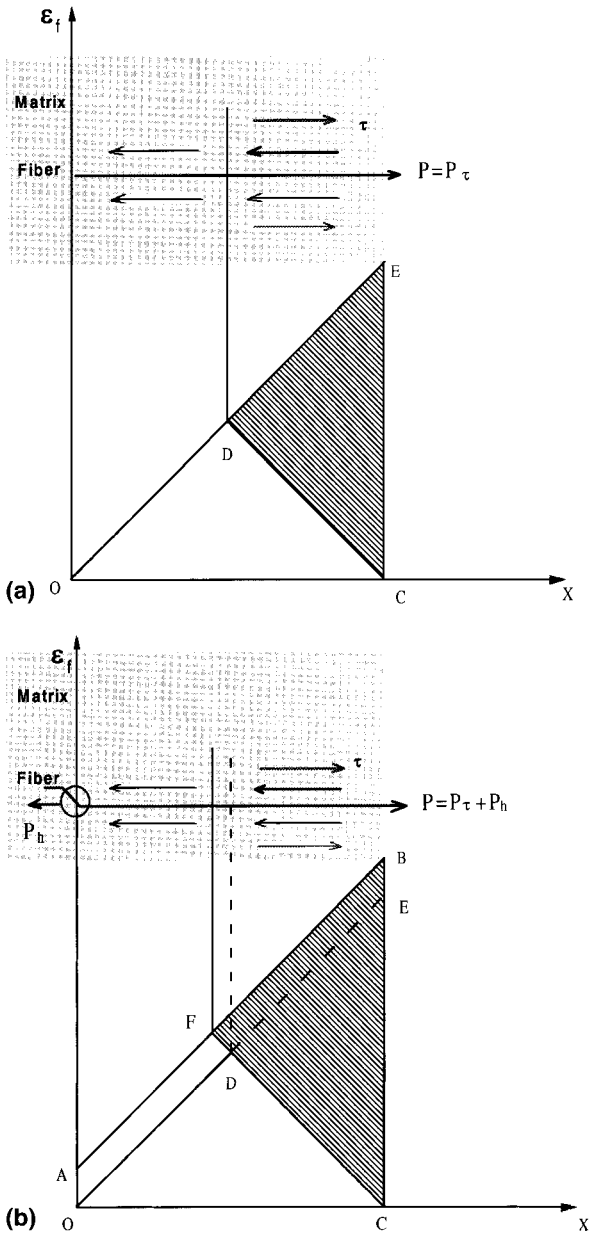

FIG. 11. Comparison of Single Fiber Pullout under Cyclic Loading between Smooth and Hooked Fibers

at the point of full fiber debonding as described above. For hooked fiber, the bridging components, in addition to the interfacial bond along the straight part, also include the mechanical action of the hooked end, as shown in Fig. 11. The amplitude of fiber pullout and slip-back under cyclic tensile load depends not only on the bond stress along the straight debonding area but also on the mechanical action P_h offered by hook. The amplitude of fiber pullout and slip-back of hooked fiber is larger than that of smooth fiber ($S_{CFBC} > S_{CDEC}$).

For 3D distributed discrete FRC materials, the amplitude of fiber pullout and slip-back is the sum of individual fibers that are of different embedded lengths and pullout states. The experimental results are shown in Fig. 4 for these two types of SFRCs. The maximum fiber bridging stress degradation will appear near the full debonding point of all fibers for SSFRC. From the experimental results shown in Fig. 7, the largest total bridging degradation, including the aggregate bridging degradation, in SSFRC occurs at a point within the maximum crack width of 0.1–0.2 mm. Before this point it increases with maximum crack width and after that it decreases. In theory (Li et al. 1993), the full debonding point of all fibers is calculated

to be at the point of maximum crack width of 0.07 mm for the mechanical and geometric parameters of the steel fiber used. Here the Cook-Gordon debonding effect (Cook and Gordon 1964; Li et al. 1993) is included. But for HSFRC, due to the hooked-end action, the amplitude of fiber pullout and slip-back gradually increases with the maximum slippage within the range of experimental investigation, and the bridging decay increases with the maximum fiber slippage represented by the maximum crack width. As the maximum crack width is <0.1 mm, because the hook action is limited, the difference on the amplitude of fiber pullout and slip-back between SSFRC and HSFRC is small. Thus, almost identical stress degradation on both materials is found [Fig. 6(a and b)].

From the test results and analysis above, we can conclude that although the hooked fiber can efficiently improve the monotonic crack bridging performance compared to smooth fibers in FRC materials, under cyclic loading, the bridging stress offered by hooked fibers is also more easy to degrade, particularly when the imposed crack opening is relatively large.

CONCLUSIONS

The crack bridging behavior of SFRC materials reinforced with two types of commercially available steel fibers, smooth and hooked-end, respectively, were investigated in the present study under uniaxial fatigue tensile load with constant amplitude between minimum and maximum crack widths. The main conclusions can be drawn as follow.

The crack bridging in SFRC materials degrades with the number of cycles under deformation controlled fatigue tensile load. The behavior of crack bridging degradation in SFRC is a fast dropping stage (within the first 10–15 cycles) with a decelerated degradation rate followed by a stable stage with an almost constant degradation rate for SSFRC or by several periods with a decelerated rate in each period for HSFRC. Faster bridging degradation is found in HSFRC than in SSFRC with the same maximum crack width and minimum load condition, particularly in the cases of maximum crack widths >0.1 mm. For SSFRC, the maximum bridging stress degradation occurs close to the full-debonding point of all fibers. Before this point, the stress degradation increases with maximum crack opening, and after that it decreases. For HSFRC, no peak degradation is found in the present investigated range of maximum crack width from 0.05 to 0.5 mm because the hook has not been totally degraded before the maximum crack width <0.5 mm. The larger the maximum crack width, the larger the bridging degradation.

The largest reduction on crack bridging stress in SSFRC and HSFRC can be >50 and >80% of the values at the first cycle after 10^5 cycles within the experimental range (i.e., the maximum crack openings between 0.05 and 0.5 mm).

Although the fiber deformation, such as hooked end fiber, can improve the monotonic crack bridging of SFRC materials significantly, this mechanical action offered by hooks will also increase the elastic slippage of fibers during fatigue loading, which in turn speeds up the bridging stress degradation. This influence becomes more pronounced with the increase of maximum crack width.

ACKNOWLEDGMENTS

This work has been supported by a grant from the Danish Ministry of Education to the Technical University of Denmark (DTU), Lyngby, Denmark, and partly by a NATO grant which supports collaboration research between the Department of Structural Engineering and Materials, DTU, and the Advanced Civil Engineering Materials Research Laboratory, University of Michigan, Ann Arbor, Mich. Support from the National Science Foundation (CMS-9872357) to the University of Michigan is gratefully acknowledged. Fruitful discussions with Dr. T. Matsumoto are gratefully acknowledged.

APPENDIX. REFERENCES

Aarre, T. (1992). ''Tensile characteristics of FRC with special emphasis on its applicability in a continues pavement,'' PhD thesis, Serie R, No. 301, Dept. of Struct. Engrg. and Mat., Technical University of Denmark, Lyngby, Denmark.

Byung, B., and Oh, H. (1986). ''Fatigue analysis of plain concrete in flexure.'' *J. Struct. Engrg*., ASCE, 112(2), 273–288.

Cook, J., and Gordon, J. E. (1964). ''A mechanism for the control of crack propagation in all brittle systems.'' *Proc., Royal Soc*., London, 282A, 508–520.

Cox, B. N., and Rose, L. R. F. (1994). ''Time-or cycle-dependent crack bridging.'' *Mech. of Mat*., 19, 39–57.

Evans, A. G., Zok, F. W., and Mcmeeking, R. M. (1995). ''Fatigue of ceramic matrix composites.'' *Acta Metall. Mat*., 43(3), 859–875.

Gopalaratnam, V. S., and Shah, S. P. (1985). ''Softening response of plain concrete in direct tension.'' *ACI J*., 82(3), 310–323.

Gylltoft, K. (1983). ''Fracture mechanics models for fatigue in concrete structures,'' PhD thesis, Div. of Struct. Engrg., Luleå University of Technology, Luleå, Sweden.

Hordijk, D. A. (1991). ''Local approach to fatigue of concrete,'' PhD thesis, Delft University of Technology, Delft, The Netherlands.

Hsu, T. T. C. (1981). ''Fatigue of plain concrete.'' *ACI J*., July–Aug., 292–305.

Johnston, C. D., and Zemp, R. W. (1991). ''Flexural influence of fiber content, aspect ratio and type.'' *ACI Mat. J*., Jul-Aug., 347–383.

Li, V. C., and Matsumoto, T. (1998). ''Fatigue crack growth analysis of fiber reinforced concrete with effect of interfacial bond degradation.'' *Cement and Concrete Compos*., 20(5), 353–363.

Li, V. C., Stang, H., and Krenchel, H. (1993). ''Micromechanics of crack bridging in fiber reinforced concrete.'' *Mat. and Struct*., Paris, 26, 486–494.

Otter, D. E., and Naaman, A. E. (1988). ''Properties of steel fiber reinforced concrete under cyclic loading.'' *ACI Mat. J*., July-Aug., 254–261.

Ramakrishan, V., Oberling, G., and Tatnall, P. (1987). ''Flexural fatigue strength of steel fiber reinforced concrete.'' *Proc., Symp*., America Concrete Institute, Detroit, 225–245.

Reinhardt, H. W., Cornelissen, A. W., and Hordijk, D. A. (1986). ''Tensile tests and failure analysis of concrete.'' *J. Struct. Engrg*., ASCE, 112(11), 2462–2477.

Rouby, D., and Reynaud, P. (1993). ''Fatigue behavior related to interface modification during cycling in ceramic-matrix fiber composites.'' *Compos. Sci. and Technol*., 48, 109–118.

Saito, M., and Imai, S. (1983). ''Direct tensile fatigue of concrete by the use of friction grips.'' *ACI J*., Sep.-Oct., 431–438.

Stang, H., and Aarre, T. (1992). ''Evaluation of crack width in FRC with conventional reinforcement.'' *Cement and Concrete Compos*., 14(2), 143–154.

Stang, H., and Zhang, J. (1994). ''Experimental determination of fatigue crack growth in fiber reinforced concrete.'' *Recent advances in experimental mechanics*, J. F. Silva Gomez et al., eds., Balkema, Rotterdam, The Netherlands, 1347–1352.

Tepfers R., and Kutti, T. (1979). ''Fatigue strength of plain, ordinary and lightweight concrete.'' *ACI J*. May, 636–652.

Wu, H. C., Matsumoto, T., and Li, V. C. (1994). ''Buckling of bridging fibers in composites.'' *J. Mat. Sci. Letters*, 13(24), 1800–1803.

Zhang, J. (1998). ''Fatigue fracture of fiber reinforced concrete—An experimental and theoretical study,'' PhD thesis, Serie R, No. 41, Dept. of Struct. Engrg. and Mat., Technical University of Denmark, Lyngby, Denmark.

Zhang, J., and Stang, H. (1997a). ''Bridging behavior and crack growth in FRC under fatigue load.'' *Proc., 5th Int. Symp. on Brittle Matrix Compos. (BMC5)*, A. M. Brandt, V. C. Li, and I. H. Marshall, eds., 143–153.

Zhang, J., and Stang, H. (1997b). ''Interfacial degradation in cement-based fibre reinforced composites.'' *J. Mat. Sci. Letters*, 16(11), 886–888.

Zhang, J., and Stang, H. (1998). ''Fatigue performance in flexure of fiber reinforced concrete.'' *ACI Mat. J*., 95(1), 58–67.